

The *Arabidopsis thaliana* Homolog of Yeast *BRE1* Has a Function in Cell Cycle Regulation during Early Leaf and Root Growth

Delphine Fleury,^{a,b,1} Kristiina Himanen,^{a,b,1} Gerda Cnops,^{a,b} Hilde Nelissen,^{a,b} Tommaso Matteo Boccardi,^{a,b} Steven Maere,^{a,b} Gerrit T.S. Beemster,^{a,b} Pia Neyt,^{a,b} Sylvester Anami,^{a,b} Pedro Robles,^c José Luis Micol,^c Dirk Inzé,^{a,b} and Mieke Van Lijsebettens^{a,b,2}

^aDepartment of Plant Systems Biology, Flanders Institute for Biotechnology, Ghent University, B-9052 Gent, Belgium

^bDepartment of Molecular Genetics, Ghent University, B-9052 Gent, Belgium

^cDivisión de Genética and Instituto de Bioingeniería, Universidad Miguel Hernández, Campus de Elche, E-03202 Elche (Alicante), Spain

Chromatin modification and transcriptional activation are novel roles for E3 ubiquitin ligase proteins that have been mainly associated with ubiquitin-dependent proteolysis. We identified *HISTONE MONOUBIQUITINATION1 (HUB1)* (and its homolog *HUB2*) in *Arabidopsis thaliana* as RING E3 ligase proteins with a function in organ growth. We show that HUB1 is a functional homolog of the human and yeast BRE1 proteins because it monoubiquitinated histone H2B in an in vitro assay. *Hub* knockdown mutants had pale leaf coloration, modified leaf shape, reduced rosette biomass, and inhibited primary root growth. One of the alleles had been designated previously as *ang4-1*. Kinematic analysis of leaf and root growth together with flow cytometry revealed defects in cell cycle activities. The *hub1-1 (ang4-1)* mutation increased cell cycle duration in young leaves and caused an early entry into the endocycles. Transcript profiling of shoot apical tissues of *hub1-1 (ang4-1)* indicated that key regulators of the G2-to-M transition were misexpressed. Based on the mutant characterization, we postulate that HUB1 mediates gene activation and cell cycle regulation probably through chromatin modifications.

INTRODUCTION

Ubiquitin is a highly conserved small protein of 76 amino acids that plays a role in proteolysis because it labels specific proteins for destruction. Polyubiquitination of these target proteins requires the concerted action of a number of proteins: a ubiquitin-activating enzyme E1 and a ubiquitin-conjugating enzyme E2 that usually work with ubiquitin ligase E3, which is required for substrate specificity (Conaway et al., 2002). E3 ubiquitin ligases belong to a large and diverse family of proteins or protein complexes that represent ~90% of the genes encoding components of the ubiquitin-proteasome pathway. The E3 ligase superfamily of *Arabidopsis thaliana* consists of >460 members that are classified based on the presence of an E6-AP C terminus, U-box, or Really Interesting New Gene (RING) domain (Stone et al., 2005). In plants, various biological processes, such as cell cycle, embryogenesis, hormone signaling, photomorphogenesis, floral devel-

opment, and senescence, are regulated by ubiquitin-dependent proteolysis (for review, see Smalle and Vierstra, 2004).

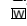
Monoubiquitination of histone H1, H2A, H2B, and H3 is necessary for meiosis, telomere silencing, transcriptional silencing, and activation and is a nontraditional function of the ubiquitination enzymes (Schnell and Hicke, 2003). In yeast (*Saccharomyces cerevisiae*) and humans, the Bre1 E3 ubiquitin ligases monoubiquitinate histone H2B. This histone H2B modification is required for transmethylation of histone H3 and thereby plays a crucial role in the formation of transcriptionally active chromatin (Wood et al., 2003; Kim et al., 2005; Zhu et al., 2005). The yeast *BRE1* gene also is involved in the control of cell size (Hwang et al., 2003).

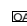
The leaf has been exploited as a model to study the genetic and environmental factors that regulate organ size and shape in multicellular organisms. Early leaf growth is mainly due to cell division processes that cease gradually from the tip to the base of the organ, from its margin to the midvein, and from the ventral to the dorsal side of the lamina (Pyke et al., 1991; Donnelly et al., 1999). Interference with early growth by modulation of cell cycle regulatory genes has resulted in changes in final leaf size and shape (Wyrzykowska et al., 2002). Later leaf growth is mainly driven by cell expansion. The availability of a collection of 94 leaf mutant loci originating from an ethyl methanesulfonate mutagenesis program (Berná et al., 1999) is an important resource to determine the genetic control of leaf growth. Many mutated genes from this collection are being cloned and their function in leaf growth analyzed in detail (Pérez-Pérez et al., 2004; Nelissen

¹ These authors contributed equally to this work.

² To whom correspondence should be addressed. E-mail mieke.vanlijsebettens@psb.ugent.be; fax 32-9-3313809.

The author responsible for distribution of materials integral to the findings presented in this article in accordance with the policy described in the Instructions for Authors (www.plantcell.org) is: Mieke Van Lijsebettens (mieke.vanlijsebettens@psb.ugent.be).

 Online version contains Web-only data.

 Open Access articles can be viewed online without a subscription. www.plantcell.org/cgi/doi/10.1105/tpc.106.041319

et al., 2005). The *histone monoubiquitination1* mutant, *hub1-1* (previously designated *ang4-1*), belongs to the *angusta* class of recessive mutants that consist of four loci characterized by reduced leaf size and narrow laminae (Berná et al., 1999; Robles and Micol, 2001). Here, we report that the *HUB1* gene encodes the functional homolog of yeast and human histone H2B-monoubiquitinating BRE1 RING E3 ligases, and we propose a role for HUB1 in the regulation of the cell cycle during early organ growth in plants.

RESULTS

hub1-1 Affects Leaf and Root Growth through Cell Proliferation

The main characteristic of the *hub1-1* (*ang4-1*) mutant of *Arabidopsis* is its small plant size and narrow leaf lamina (Figures 1 and 2A, Table 1). The reduced leaf area in the *hub1-1* mutant was confirmed by morphological measurements of the fully expanded leaves 1 and 2 that had a significantly decreased lamina length and width, petiole length, and total lamina and petiole lengths (Table 1). The lamina area of mature first and second leaves of *hub1-1* was reduced to 55% of that of the wild-type Landsberg *erecta* (*Ler*) (Table 1). The length:width ratio was significantly increased, reflecting a much stronger reduction in width than in length of the blade (Table 1). Similar observations were made on leaf 6 (Cookson et al., 2005). The *hub1-1* mutation also affected rosette growth, reducing fresh and dry weight at flowering by 40 and 39%, respectively (Figure 2B). To investigate whether a defect of cell proliferation and/or cell expansion is responsible for the growth defects of the *hub1-1* mutant leaves, the number of palisade cells was counted in serial sections at the widest position of mature first and second leaves. The number of palisade cells across *hub1-1* lamina (31 ± 4 cells; average \pm SD, $n = 3$) was 44% that of those in *Ler* (70 ± 4 cells), resulting in narrow leaf shape of the *hub1-1* mutant (Figure 2C). In addition to reduced cell numbers, distribution and size of the mesophyll cells were irregular with some enlarged cells and the air spaces were increased (Figure 2D). In leaf 6, similarly reduced cell numbers had been observed in the epidermal cell layer (Cookson et al., 2005). Thus, the main cause of the reduced leaf size in *hub1-1* was a decrease in cell numbers. To verify whether the *hub1-1*

mutation influenced the growth of other organs, the length of the primary roots was measured in vitro during early seedling development. The *hub1-1* primary roots grew much more slowly than those of the wild-type *Ler* (Figure 2E). To investigate whether the effect was due to morphogenetic defects, the root apical meristems were stained with propidium iodide and 4',6-diamidino-2-phenylindole and analyzed by confocal microscopy. No differences between *hub1-1* and *Ler* were seen regarding cellular organization or cell wall formation (see Supplemental Figures 1A to 1D online). A promoter- β -glucuronidase fusion construct with the B-type cyclin *CYCB1;1* is a powerful tool to monitor mitotic activity in roots (Himanen et al., 2002) and was transformed into *hub1-1* and *Ler* to evaluate the meristem size and activity of *hub1-1* roots. The area of the β -glucuronidase staining in the root tips had a clearly reduced meristem size (by 50%) for *hub1-1* (see Supplemental Figures 1E and 1F online). To investigate the cause of this growth reduction, root growth was analyzed kinematically. The root growth of young seedlings is often accelerated because of the increment of the number of dividing cells in the growth zone (Beemster and Baskin, 1998). As expected from the reduced meristem size, the root growth rate of *hub1-1* was severely reduced and no acceleration of growth took place (Figure 3A). To verify whether the reduction of root growth rate was caused by reduced cell production as suggested by the reduced meristem size or by reduced cell expansion, the length of cortex cells was measured. The average mature cortex cell length was significantly ($P < 0.001$) reduced from 171 μ m in *Ler* to 104 μ m in *hub1-1*, whereas the cell production per hour had decreased by 65%, from 1.26 in *Ler* to 0.44 in *hub1-1* (Figure 2F). Thus, *hub1-1* affected root growth by altering both cell production in meristem and postmitotic cell expansion.

hub1-1 Affects Cell Division Rate but Not Developmental Timing in Leaves

To examine the changes in cell division and expansion underlying the growth phenotype, we performed a kinematic analysis (Beemster et al., 2005) on epidermal cells of leaves 1 and 2 of in vitro-grown mutant and wild-type plants. Five days after sowing (DAS), leaf blade area and epidermal cell number were similar in *Ler* and *hub1-1* (Figures 3B and 3C), but both parameters increased more slowly in *hub1-1* than in *Ler* between 5 to 10 DAS, ultimately resulting in a reduced leaf size (47%) and number of



Figure 1. Plant Phenotypes of the *hub1* and *hub2* Mutants and the Corresponding Wild Types, *Ler* and *Col*, Grown in Soil in a Growth Chamber.

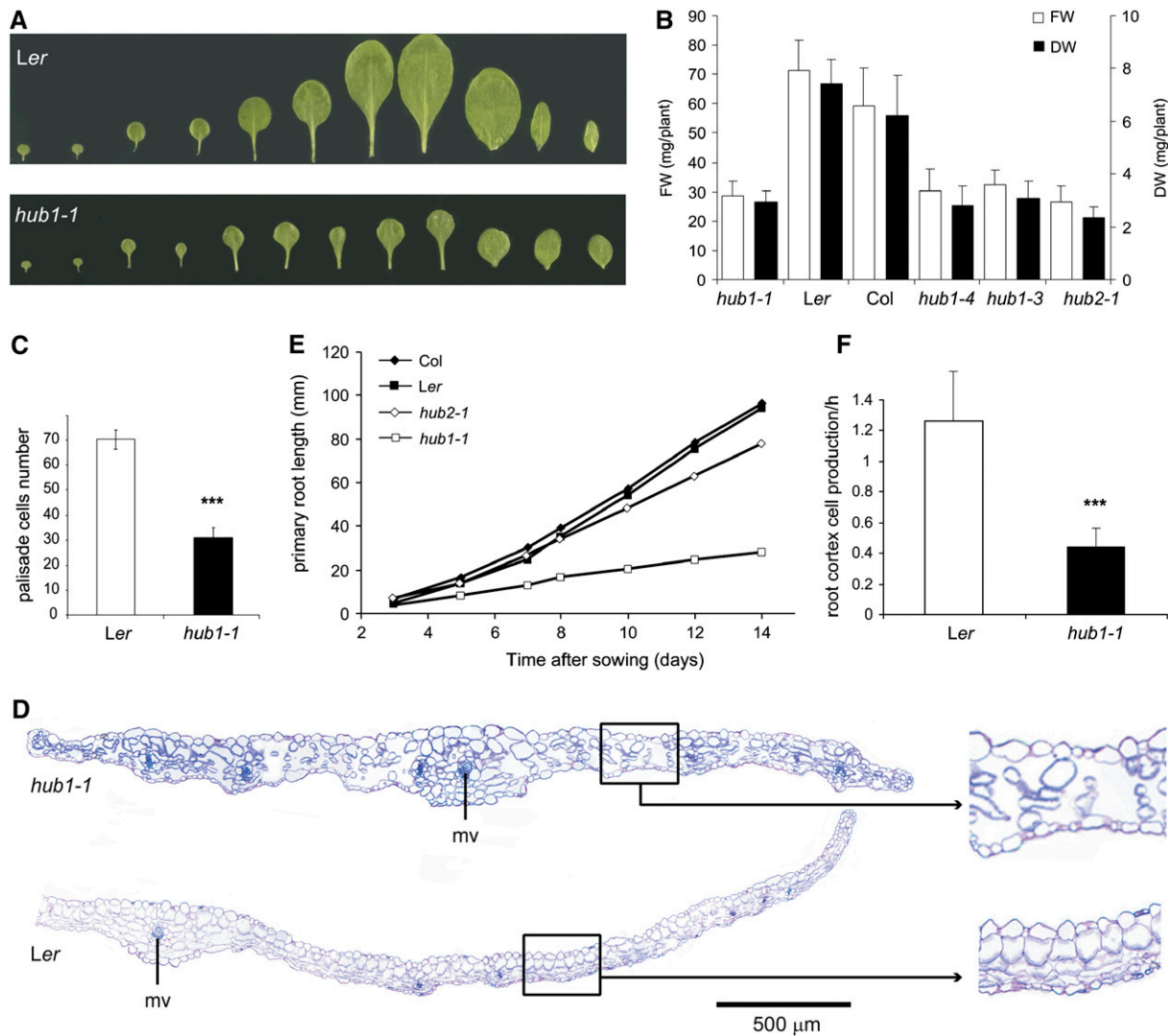


Figure 2. Leaf and Root Phenotypes of *hub1* and *hub2*.

(A) Juvenile and adult fully expanded leaves of *Ler* (top panel) and *hub1-1* (bottom panel).

(B) Rosette weight of *hub1-1*, *hub1-4*, *hub1-3*, *hub2-1*, *Ler*, and *Col* plants grown in soil ($n = 48$ plants) and harvested at inflorescence emergence stage. FW, fresh weight; DW, dry weight. Bars indicate mean \pm SD.

(C) Absolute palisade cell number across half of the first and second expanded leaves ($n = 3$). Bars indicate mean \pm SD. ***, Statistical difference at $P < 0.001$ from the t test.

(D) Transverse section through the central part of the first leaf of plants (26 DAS) grown in vitro. mv, midvein.

(E) Primary root growth kinetics of mutants *hub1-1* and *hub2-1* and wild types *Ler* and *Col* grown under in vitro conditions ($n = 8$).

(F) Root cortex cell production per hour in *Ler* and *hub1-1* seedlings grown in vitro. Bars indicate mean \pm SD ($n = 1200$).

epidermal cells (48%) in *hub1-1* leaves by day 18, when the growth phase ended in both lines. The relative leaf expansion rate (RLER) is the leaf area produced per unit of time, and the cell division rate (CDR) is the total number of cells produced per unit of time and per meristematic cell. Between 5 and 10 DAS, the RLERs and the CDRs were lower but decreased more slowly in *hub1-1* than in the wild type (Figures 3D and 3E). Consequently, RLERs and CDRs became similar in *hub1-1* and *Ler* from 10 DAS. Thus, the *hub1-1* mutation altered the cell division and the leaf expansion rates during the proliferation phase of leaf develop-

ment but did not affect the duration of proliferation or leaf expansion.

The average cell cycle duration is the time between two successive phases of mitosis and is calculated as the inverse of CDR. At 5 DAS, the estimated average cell cycle duration was 44% longer in *hub1-1* (20.6 h) than in *Ler* (14.1 h). Hence, the *hub1-1* mutation affected the cell divisions by increasing the cell cycle duration during early stages of leaf development.

The average cell (or organ) size depends on the balance between cell division and expansion and on the size at which

Table 1. Morphological Data of Expanded Leaves of *hub1-1* and *Ler* Grown in Vitro (P Value from a *t* Test with *n* > 18 Plants)

Trait	<i>Ler</i>	<i>hub1-1</i>	P Value
Lamina length (mm)	5.33 ± 0.41	4.73 ± 0.45	<0.001
Lamina width (mm)	4.88 ± 0.28	3.30 ± 0.52	<0.001
Petiole length (mm)	3.76 ± 0.29	3.16 ± 0.46	<0.001
Lamina and petiole length (mm)	9.09 ± 0.56	7.89 ± 0.72	<0.001
Lamina length/width ratio	1.09 ± 0.04	1.46 ± 0.20	<0.001
Lamina area (mm ²)	19.32 ± 2.52	10.67 ± 2.40	<0.001

cells divide. At 5 DAS, the cells of *hub1-1* were significantly larger than those of *Ler*; however, after 7 DAS, no differences in average epidermal cell area could be observed between *Ler* and *hub1-1*, indicating that *HUB1* did not modify the balance between RLERs and CDRs and that the reduced epidermal CDR was not compensated by an increased cell size.

Stomata originate by asymmetric cell divisions that occur late in leaf development. Thus, high stomatal index reflects mitotic competence of the leaf epidermal cells (Boudolf et al., 2004a) as well as developmental exit from cell cycle, which under normal conditions starts from the tip to the base of the leaf in *Arabidopsis* (Donnelly et al., 1999). By contrast, low stomatal index would indicate premature exit from cell cycle. Furthermore, cells that have gone through rounds of endocycles have exited the mitotic cycle and cannot initiate stomata anymore. The stomatal index was consistently reduced in all *hub1-1* when compared with *Ler* samples, suggesting that a proportion of leaf epidermal cells of *hub1-1* exit the mitotic cell cycle early (Figure 3F). The stomatal index (i.e., the fraction of epidermal cells that are guard cells) increased more slowly in *hub1-1* than in *Ler* between 5 and 8 DAS, with final values of 0.23 and 0.35 on average for *hub1-1* and *Ler*, respectively. As a result, in mature leaves of *hub1-1*, fewer stomata were present, a difference that originated at the same time when division rates were changed. Thus, the *hub1-1* mutation alters cell division in both pavement and stomatal precursor cells.

hub1-1 Affects G2-to-M Transition and Endoreduplication

During *Arabidopsis* leaf development, the cell cycle occurs in two different modes: mitosis and endoreduplication (Inzé and De Veylder, 2006). To investigate the effect of the *hub1-1* mutation on cell cycle progression, we measured the ploidy level of wild-type and mutant leaves throughout their development by means of flow cytometry. The ploidy levels can reveal changes in the relative duration of G1 and G2 phases during mitotic cell division, indicated by the fraction of cells with a 2C and 4C DNA content. Already at 8 DAS, a shift was observed in the G1-to-G2 cell populations in the *hub1-1* mutant compared with the *Ler* wild type (Figures 4A and 4B). The population of 4C cells was significantly increased at the expense of the 2C fraction (2C = 46.2% and 4C = 44.0%), whereas in the wild type, the number of cells in 4C (33.8%) was only half those in 2C (66.2%). Thus, the increased cell cycle duration in *hub1-1* might be associated with an increased duration of G2 and a block at the G2-to-M transition point of the cell cycle.

Endoreduplication is an alternate version of the cell cycle in which the nuclear DNA is replicated without mitosis or cytokinesis and is a common process in plants for increasing the nuclear ploidy (>8C) and possibly cell size (Inzé and De Veylder, 2006). From the earliest stage on (8 DAS), in the *hub1-1* mutant, the endocycle was enhanced by already 10% of 8C cells, while this level was reached only at 13 DAS in *Ler*. Consequently, in mature leaves of the *hub1-1* mutant, >4% of the cells contained a ploidy level of 32C, whereas this fraction was absent in those of *Ler*. Hence, when *HUB1* is mutated, cells appear to arrest in the G2-to-M phase of the mitotic cycle and proceed into endocycles instead. In both lines, cell cycle activity ended, as evidenced by a stable DNA distribution, at around 18 DAS, corresponding to the end of growth. To confirm that these effects were not leaf specific, flow cytometry was performed on roots, hypocotyls, and first leaves of *hub1-1* and *Ler* at 12 DAS. The ploidy levels obtained for the root and hypocotyls were comparable to those of the first leaves with a shift of 2C/4C cells and higher endoreduplication levels in *hub1-1* (see Supplemental Figure 2 online). Taken together, these results suggest that *HUB1* promotes continuation of the mitotic cell cycle at the G2-to-M transition point.

Transcriptome Analysis of *hub1-1* Shoot Apices

To get an insight into the cell cycle effects in *hub1-1* and to explore other possible molecular processes underlying the cell proliferation defects observed in the meristematic tissues of *hub1-1*, we conducted a genome-wide expression analysis on the shoot apices of young plants with microarrays (see Methods). With the PerfectMatch-MisMatch comparison, 14,460 and 14,874 expressed genes were detected in *Ler* and in *hub1-1*, respectively. The statistical analysis identified a total of 1758 differentially expressed genes between *hub1-1* and *Ler* at Holm's *P* < 0.05 (i.e., 12% of the expressed genes), among which 53.1% were downregulated and 46.9% were upregulated with fold change expression ranging from 0.007 to 0.745 and 1.3 to 153.8, respectively.

To characterize biological processes, the up- and downregulated genes were analyzed for gene ontology (GO) (Maere et al., 2005). A significantly high number of genes differentially expressed in *hub1-1* were related to cell cycle (24 genes) and cytokinesis (31 genes). These two classes of differentially regulated genes were not present in microarray data sets of the *elongata* class of narrow leaf mutants (Nelissen et al., 2005) analyzed in the same experiment (D. Fleury, unpublished data). Because of the proliferation defect observed in *hub1-1* leaves, we focused our analysis on these two classes of genes.

Among the downregulated genes in *hub1-1*, cell fate specification, histone phosphorylation, regulation of progression through cell cycle, mitotic cell cycle, and microtubule-based movement genes were significantly overrepresented. For cellular components, the underexpressed genes in *hub1-1* were significantly related to myosin, spindle, microtubule, and phragmoplast (data not shown). Among the 82 genes with a peak expression in mitosis (Menges et al., 2005), 66 were significantly downregulated in the *hub1-1* mutant, of which 37 genes had a known function in mitosis (Table 2).

Among the genes related to the mitotic cell cycle, A-type and B-type cyclins and three B-type cyclin-dependent kinases

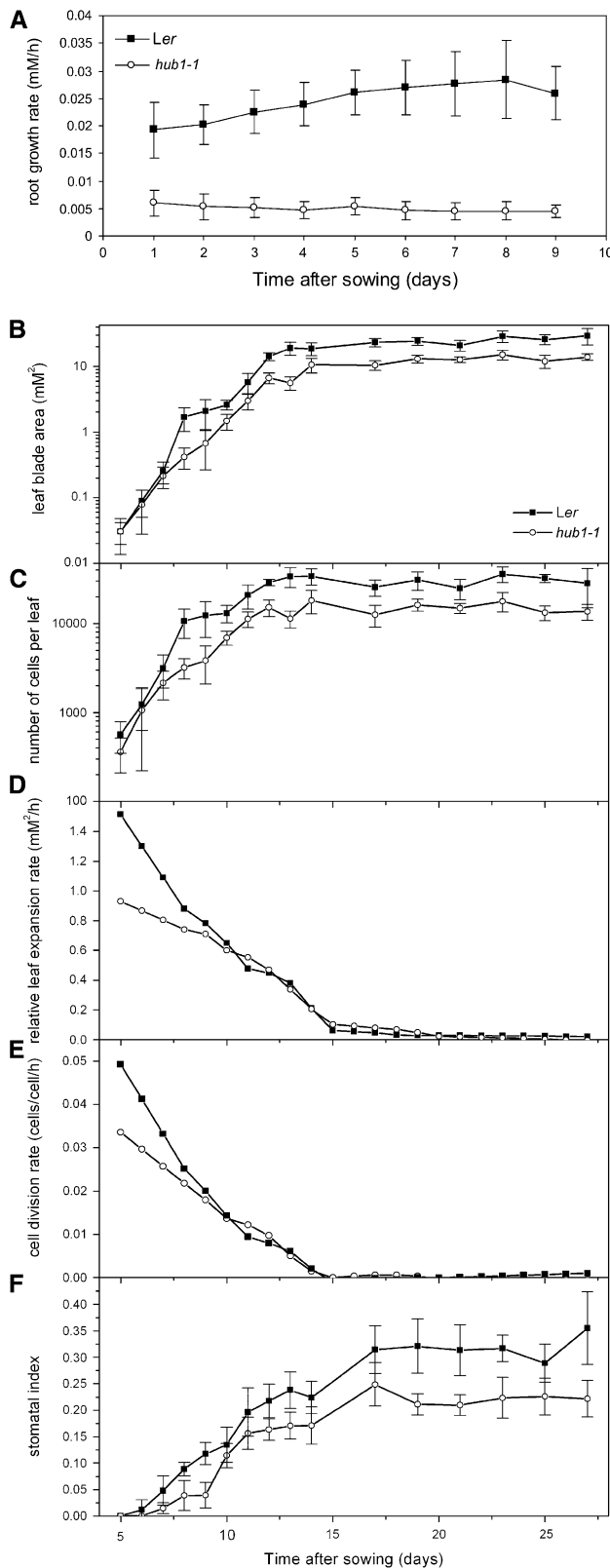


Figure 3. Kinematic Analysis of Leaf and Root Growth of the First Leaf Pair of the Wild Type *Ler* and the *hub1-1* Mutant.

(CDKBs) are involved in the regulation of the G2-to-M transition (Inzé and De Veylder, 2006). Of the cytokinesis-related genes, 26 kinesins or kinesin-like genes and genes related to microtubule and myosin were downregulated in *hub1-1*, among which are the kinesins *HINKEL* (*NACK1*) and *TETRASPORE* (*NACK2*), syntaxin (*KNOLLE*), and *MAP63-3* (*PLEIADE*). The transcriptome data show that *HUB1* affects cell cycle regulation and, more specifically, the mitosis and cytokinesis processes in proliferating tissue, in agreement with the G2-to-M inhibition suggested by the kinematic and flow cytometric data.

Interestingly, the analysis of upregulated genes also identified GO categories related to cytokinesis. Two upregulated genes were involved in callose synthesis during cell plate formation: *ENDOXYLOGLUCAN TRANSFERASE* (*DECOY*) and *CALLOSE SYNTHASE1*, both of which are implicated in cell wall/cell plate formation (Table 3). Furthermore, the *SIAMESE* (*SIM*) gene, with a function in endoreduplication during trichome formation on leaves, and the E2F dimerization partner (*DPa*) transcription factor gene were upregulated (Table 3). Finally, some overexpressed genes in *hub1-1* were related to meristem development, such as the homeodomain genes *KNOTTED1-LIKE2* (*KNAT2*), *KNAT6*, *SHOOT MERISTEMLESS*, and 12 *NO APICAL MERISTEM* genes (Table 3). A total of 13 homeotic genes had an altered expression in *hub1-1*, among which were two SNF2 proteins (At3g63950 and At1g05480) and a BRAHMA-like protein (At3g06010) of the Polycomb group of proteins in fruitfly (*Drosophila melanogaster*). Other categories downregulated in *hub1-1* comprised genes involved in carboxylic acid metabolism, fatty acid metabolism, lipid biosynthesis, vitamin biosynthesis, cofactor biosynthesis, chlorophyll biosynthesis, transfer RNA metabolism, photosynthesis, and protein targeted to chloroplast (Figure 5). Biological processes, such as response to stress, proton transport, cell redox homeostasis, hexose metabolism, cellular respiration, and cofactor catabolism, were significantly overexpressed in *hub1-1*. Thus, besides effects on meristem development and cell cycle control, the *hub1-1* mutant was generally defective in plant metabolism at the transcriptional level, possibly reflecting secondary effects on the observed growth defects.

***HUB1* and Its Homolog Encode RING Finger Proteins, Orthologous to the Yeast and Human BRE1 Protein**

The *hub1-1* allele was obtained by mutagenesis of the *Arabidopsis* ecotype *Ler* with ethyl methanesulfonate and was originally designated *ang4-1* (Berná et al., 1999). Map-based cloning of the gene was done on an F2 population derived from a cross *hub1-1/hub1-1* × Columbia (*Col*) according to Peters et al. (2004). First, the *hub1-1* mutation was mapped with amplified fragment length polymorphism markers to a 293-kb interval on

(A) Root growth rate.
(B) Leaf lamina area.
(C) Epidermal cell number on the abaxial side of the leaf.
(D) Relative leaf expansion rate.
(E) Average CDRs of the epidermal cells on the abaxial side of the leaf.
(F) Stomatal index on the abaxial side of the leaf.
Error bars indicate SD ($n = 5$).

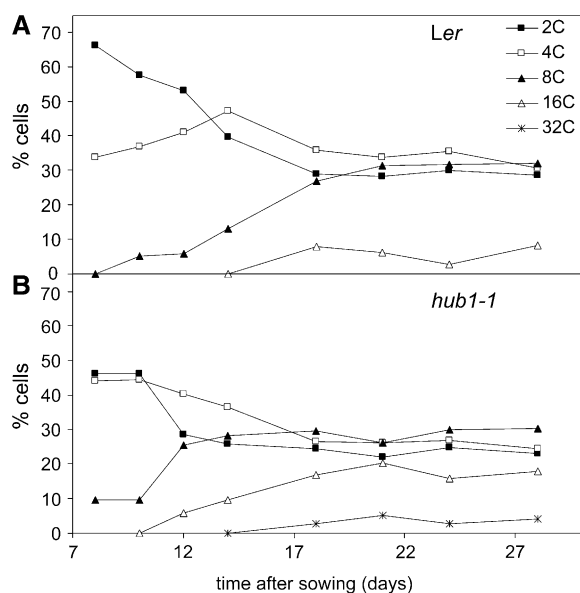


Figure 4. Effect of *hub1-1* on Nuclear DNA Content during the Development of the First Leaf Pair by Flow Cytometry Analysis.

(A) *Ler*.
(B) *hub1-1* mutant.

chromosome 2 (Figure 6A) that was then reduced to 27 kb by further linkage analyses with insertion/deletion (InDel) and single nucleotide polymorphism (SNP) markers. The four genes in this interval (At2g44940, At2g44950, At2g44970, and At2g44980) were amplified by PCR and sequenced in *Ler* and the *hub1-1* mutant. A single base pair change (C to T) occurred at position 5183 (<http://www.arabidopsis.org>) in the genomic sequence of At2g44950, changing the last codon of exon 16 from CAG (Gln) into the stop codon TAG, with a truncated protein of 711 amino acids compared with the 878 amino acids of the wild-type protein. These data were confirmed through the sequence analysis of the *hub1-1* cDNA. HUB1 contains a RING finger domain (PF00097) at position 826 to 864 and is classified as an HCa-RING-type protein (Stone et al., 2005). RING finger domains are specialized types of Zn finger domains of 40 to 60 residues that bind two atoms of zinc and are known to mediate protein–protein interactions. The *hub1-1* mutation created a truncated protein lacking the RING domain. Both the *hub1-1* (*ang4-1*) mutation and the *rd4* mutation (Peeters et al., 2002; Liu et al., 2007) were identified in At2g44950.

Previously, the *HUB1* gene was classified as a BRE1 homolog (Hwang et al., 2003; Stone et al., 2005). In multicellular organisms, two copies of the BRE1 protein are present, such as STARING and XP_232995 in rat (*Ratus norvegicus*) (Chin et al., 2002) and RNF40 and RNF20 in human (Zhu et al., 2005). In *Arabidopsis*, another BRE1 homolog belonging to the same class of RING finger proteins has also been identified by Chin et al. (2002) as an 899–amino acid protein (At1g55250) and a shorter 384–amino acid protein (At1g55255) by Stone et al. (2005). Although the annotation of At1g55250 and At1g55255 as two different genes was supported by The Institute for Genome

Research and The Arabidopsis Information Resource, we suspected annotation errors based on sequence homology to At2g44950. Therefore, we performed RT-PCR with primers extending over the large putative intergenic region (or putative large intron) and detected a transcript that spanned both annotated genes, demonstrating that they indeed represented a single gene, which was designated *HUB2*. At the protein level, HUB1 and HUB2 were 28% identical and shared 50% of similar amino acids. HUB1 and HUB2 shared 13 and 12.5% identity and 31 and 29% similarity with yeast BRE1, respectively. As in *Arabidopsis*, the homology between HUB1 and HUB2 was higher with the BRE1 co-orthologs in multicellular organisms than with that of the yeast BRE1 (for example, HUB1 shares 23% identity and 43% similarity with STARING).

From public collections, two insertional mutations in At2g44950 were obtained, which we designated *hub1-4* and *hub1-3* with T-DNA insertions in exons 19 and 6, respectively (Table 4). In *hub1-4* and *hub1-3* mutants, growth was defective compared with that of the Col wild type. The mutants were reduced in size (Figure 1) and had pale-green laminae with an irregular blade surface and thinner inflorescence stems (Figure 1), but root growth was not visibly reduced. Furthermore, the fresh weight of *hub1-4* and *hub1-3* was 51 and 55% of that of Col, respectively (Figure 2B). The weaker phenotype of the *hub1-4* and *hub1-3* mutants compared with that of *hub1-1* could be due to the genetic background (Col versus *Ler*) because a less severe *hub1-1* phenotype was also observed in the F2 mapping population (mixed Col/*Ler* background). A similar observation of stronger phenotypes in *Ler* than in Col backgrounds had already been observed for other leaf mutants (Horiguchi et al., 2005; Nelissen et al., 2005).

To confirm that *hub1-1* corresponds to a mutation in the At2g44950 gene, we performed allelism tests between *hub1-1*, and *hub1-4* and *hub1-3* (Table 4), which contain a resistance marker for kanamycin and sulfadiazine, respectively. Crosses between *hub1-1* (female), and *hub1-4* (male) and *hub1-3* (male) yielded 97 and 38 F1 seedlings resistant to kanamycin and sulfadiazine, respectively, which is the result of successful crosses. In addition, the presence of the *hub1-1* allele in these F1 seedlings was verified with a derived cleaved amplified polymorphic sequence (dCAPS) marker. The phenotypes of the F1 seedlings, with verified heterozygous genotypes, were scored. The phenotypes of the *hub1-1/hub1-4* and *hub1-1/hub1-3* F1 seedlings were most similar to those of the *hub1-1* homozygous parent, especially for the short roots; in addition, leaves were narrow and slightly reticulated as in both parents (Figure 6B). Taken together, these data confirmed that *hub1-1*, *hub1-4*, and *hub1-3* were allelic and that *HUB1* corresponded to At2g44950. The *hub1-1* mutant was complemented with a Gateway construct (Karimi et al., 2002) of p35S-*HUB1* that was transformed in *hub1-1* by floral dip (Clough and Bent, 1998). A partial restoration of the root growth, leaf size, and chlorophyll content was obtained in homozygous F3 lines with one T-DNA copy (Figure 6C).

The BRE1 Homologs *HUB1* and *HUB2* Act Genetically in the Same Pathway

A *hub2-1* knockout line was obtained from the Genome Analysis of the Plant Biological System catalog (GABI-Kat), and its T-DNA

Table 2. Downregulated Genes in *hub1-1* Compared with the *Ler* Wild Type

Fold Change	P Value	Gene Code	Gene Description	Phase	GO Category
0.113	3.23E-03	At4g38950	Kinesin motor family protein		Microtubule-based movement
0.154	8.80E-05	At5g51600	Microtubule-associated protein PLEIADE (PLE/MAP65/ASE1)	M	Cytokinesis by cell plate formation
0.175	4.00E-04	At2g25880	Aurora-like kinase 1 (ALK1)	M	Protein amino acid phosphorylation
0.182	5.59E-03	At3g27920	Trichome differentiation protein / GLABROUS1 protein (GL1)		Gibberellic acid-mediated signaling
0.184	3.12E-03	At3g23670	Phragmoplast-associated kinesin-related protein, putative	M	Microtubule-based movement
0.184	1.29E-03	At5g55520	Kinesin-like	M	Biological process unknown
0.184	6.82E-03	At1g63100	SCARECROW transcription factor (SCR)		Regulation of transcription
0.190	7.79E-05	At2g33560	Spindle checkpoint protein-related	M	Biological process unknown
0.191	1.66E-05	At1g08560	Syntaxin-related protein KNOLLE (KN)/syntaxin 111 (SYP111)	M	Intracellular protein transport
0.192	1.95E-04	At3g17360	Kinesin motor protein-related		Microtubule-based movement
0.195	1.26E-08	At5g02370	Kinesin motor protein-related	M	Cytoskeleton organization and biogenesis
0.197	3.60E-04	At3g22880	Meiotic recombination protein, putative		Meiosis
0.204	7.22E-04	At3g25980	Mitotic spindle checkpoint protein, putative (MAD2)	M	Mitotic spindle checkpoint
0.205	1.32E-03	At4g26660	Kinesin-like	M	Biological process unknown
0.205	1.97E-04	At1g18370	Kinesin protein HINKEL (NACK1)	M	Microtubule-based movement
0.214	9.29E-05	At4g32830	Aurora-like kinase 2 (ALK2)	M	Histone phosphorylation
0.218	2.63E-05	At3g10310	Kinesin motor protein-related		Microtubule-based movement
0.219	1.27E-03	At4g14330	Phragmoplast-associated kinesin-related protein (PAKRP2)		Microtubule-based movement
0.219	3.00E-05	At3g20150	Kinesin motor family protein	M	Microtubule-based movement
0.229	4.96E-03	At3g43210	Kinesin TETRASPORE (TES/NACK2)		Male meiosis cytokinesis
0.235	2.16E-03	At5g67270	Microtubule-associated EB1 family protein	M	Cortical cytoskeleton organization and biogenesis
0.238	3.43E-04	At5g13840	WD-40 repeat family protein (CCS52b)	M	Signal transduction
0.242	3.77E-04	At3g27330	Zinc finger (C3HC4-type RING finger) family protein	M	Protein ubiquitination
0.249	2.29E-02	At4g05190	Kinesin-like protein A, putative	M	Microtubule cytoskeleton organization and biogenesis
0.250	3.93E-03	At2g28620	Kinesin motor protein-related	M	Microtubule-based movement
0.258	5.08E-04	At1g34460	Cyclin (CYCB1;5)	M	Regulation of progression through cell cycle
0.258	5.65E-03	At3g51280	Male sterility MS5, putative	M	
0.266	1.78E-02	At3g44050	Kinesin motor protein-related		Microtubule-based movement
0.270	1.69E-03	At4g35620	Cyclin (CYCB2;2)	M	Regulation of progression through cell cycle
0.271	2.22E-03	At2g26760	Cyclin (CYCB1;4)	M	Regulation of progression through cell cycle
0.272	1.57E-03	At4g33260	WD-40 repeat family protein	M	Signal transduction
0.272	9.52E-04	At2g37420	Kinesin motor protein-related		Microtubule-based movement
0.280	1.97E-04	At4g21270	Kinesin-like protein A (KATA) male meiotic spindle assembly (sensu Viridiplantae)		
0.280	3.00E-03	At4g33400	Defective embryo and meristems protein-related (DEM)	M	N-terminal protein myristoylation
0.290	2.78E-03	At5g60930	Chromosome-associated kinesin, putative	M	Microtubule-based movement
0.291	4.06E-06	At1g72250	Kinesin motor protein-related	M	Microtubule-based movement
0.292	1.09E-03	At1g02730	Cellulose synthase family protein	M	Cellulose biosynthesis
0.297	2.35E-04	At1g76310	Cyclin (CYCB2;4)	M	Regulation of progression through cell cycle
0.298	1.54E-04	At2g36200	Kinesin motor protein-related		Microtubule-based movement
0.307	3.20E-03	At5g48460	Fimbrin-like protein, actin interacting protein		Biological process unknown
0.307	7.58E-03	At2g22610	Kinesin motor protein-related	M	Microtubule-based movement
0.309	5.00E-03	At1g44110	Cyclin (CYCA1;1)	M	Regulation of progression through cell cycle
0.313	1.68E-04	At5g56580	Mitogen-activated protein kinase kinase (ATMKK6)		Protein amino acid phosphorylation

(Continued)

Table 2. (continued).

Fold Change	P Value	Gene Code	Gene Description	Phase	GO Category
0.320	3.21E-04	At1g69400	Transducin WD-40 repeat family protein/mitotic checkpoint protein, putative	M	Nucleotide binding
0.337	1.44E-04	At3g04260	BC010 (E2Fb binding protein)		Regulation of transcription
0.339	4.23E-04	At4g05520	Calcium binding EF hand family protein, calcium ion binding		
0.341	5.19E-05	At1g20930	Cyclin-dependent kinase (CDKB2;2)	M	M-phase of mitotic cell cycle
0.346	1.23E-03	At5g46880	Homeobox-leucine zipper family protein		Regulation of transcription, DNA-dependent
0.350	7.62E-03	At1g79840	Homeobox-leucine zipper protein 10 (HB-10) (GLABRA2)		Cell fate specification
0.357	1.47E-02	At5g23910	Kinesin motor protein-related	M	Microtubule-based movement
0.362	8.10E-06	At1g76540	Cyclin-dependent kinase (CDKB2;1)	M	G2-to-M transition of mitotic cell cycle
0.369	7.64E-03	At1g16330	Cyclin (CYCB3;1)	M	Regulation of progression through cell cycle
0.373	1.89E-03	At4g14150	Phragmoplast-associated kinesin-related protein (PAKRP1)		Microtubule-based movement
0.373	7.34E-03	At2g38620	Cyclin-dependent kinase (CDKB1;2), G2-to-M specific		Regulation of progression through cell cycle
0.379	5.68E-04	At3g01330	Transcription factor DEL3, E2F-DP like repressor		Regulation of transcription
0.381	3.33E-04	At1g54960	NPK1-related protein kinase, putative (ANP2)		Cytokinesis
0.385	4.40E-02	At5g46910	Transcription factor jumonji (jmi) family protein		Regulation of transcription
0.386	1.76E-02	At1g49910	WD-40 repeat family protein/mitotic checkpoint protein, putative		Biological process unknown
0.392	3.61E-03	At5g54670	Kinesin-like protein C (KATC)		Microtubule-based movement
0.407	1.33E-02	At1g59540	Kinesin motor protein-related	M	Microtubule-based movement
0.429	6.52E-04	At5g63950	SNF2 domain-containing protein; DNA repair (meiosis)		Helicase activity
0.431	3.73E-04	At3g53900	Uracil phosphoribosyltransferase; interacts with KRP5		Nucleoside metabolism
0.451	3.73E-04	At1g05230	Homeobox-leucine zipper family proteinregulation of transcription, DNA-dependent		
0.455	4.18E-03	At4g14770	CPP1-related transcription factor family (E2Fa-DPa induced)		Regulation of transcription
0.455	1.43E-02	At2g29550	Tubulin β -7 chain (TUB7)		Microtubule-based process
0.459	3.61E-02	At4g34610	Homeodomain-containing protein regulation of transcription		
0.464	1.45E-03	At2g22800	Homeobox-leucine zipper protein 9 (HAT9)		Regulation of transcription
0.468	1.97E-05	At3g19820	Cell elongation protein/DWARF1/ DIMINUT (DIM)		Brassinosteroid biosynthesis
0.493	2.66E-02	At1g20590	Cyclin (CYCB2;5), G2-to-M specific	M	Regulation of progression through cell cycle
0.495	9.60E-03	At2g37080	Myosin heavy chain-related		
0.509	7.67E-04	At1g50010	Tubulin α -2/ α -4 chain (TUA2)		Microtubule-based process
0.512	1.02E-02	At3g19590	WD-40 repeat family protein/mitotic checkpoint protein, putative	M	Biological process unknown
0.512	4.08E-02	At1g75820	CLAVATA1 receptor kinase (CLV1)		Regulation of meristem organization
0.533	3.63E-02	At2g01430	Homeobox-leucine zipper protein 17 (HB-17)		Regulation of transcription
0.623	2.77E-02	At3g06010	Homeotic gene regulator, putative, similar to Brahma protein		Biological process unknown

Data were obtained from the ATH1 microarray experiment with RNA from shoot apex of young plants grown under in vitro conditions. The P values were calculated according to a Bayesian test of linear model and corrected by the Holm's method. M, mitosis specifically expressed genes (Menges et al., 2005).

Table 3. Upregulated Genes in *hub1-1* Compared with *Ler*

Fold Change	P Value	Gene Code	Gene Description	GO Category
37.69	2.34E-03	At3g04070	No apical meristem (NAM) family protein	Regulation of transcription
24.63	1.66E-08	At5g18270	No apical meristem (NAM) family protein	Regulation of transcription
17.95	5.09E-09	At1g05480	SNF2 domain-containing protein	Regulation of transcription
15.26	4.58E-09	At1g32870	No apical meristem (NAM) family protein	Regulation of transcription
5.63	2.98E-08	At3g10500	No apical meristem (NAM) family protein	Regulation of transcription
5.03	4.96E-08	At3g13210	Crooked neck protein, putative cell cycle protein	
4.82	2.98E-06	At2g18060	No apical meristem (NAM) family protein	Regulation of transcription
4.80	4.23E-05	At5g64060	No apical meristem (NAM) family protein	Regulation of transcription
4.59	9.95E-07	At5g14000	No apical meristem (NAM) family protein	Regulation of transcription
4.45	2.66E-02	At5g53980	Homeobox-leucine zipper family protein	Regulation of transcription
3.49	6.37E-07	At1g62360	Homeobox protein SHOOT MERISTEMLESS (STM)	Regulation of transcription
3.43	3.97E-02	At1g02220	No apical meristem (NAM) family protein	Regulation of transcription
3.18	1.31E-02	At3g53230	Cell division cycle protein 48 (CDC48), putative	Nucleotide binding
3.16	6.31E-05	At5g13180	No apical meristem (NAM) family protein	Regulation of transcription
3.14	8.62E-05	At5g66130	Cell cycle checkpoint protein-related (ATR17)	
2.83	3.82E-03	At5g27950	Kinesin motor protein-related	Microtubule-based movement
2.72	1.13E-02	At3g03060	AAA-type ATPase family protein (CDC48-like)	
2.62	9.77E-04	At1g70510	Homeobox protein knotted-1 like 2 (KNAT2) (K1)	Specification of carpel identity
2.62	1.12E-02	At2g16700	Actin-depolymerizing factor 5 (ADF5)	Biological process unknown
2.53	3.51E-02	At5g04470	SIAMESE protein	Biological process unknown
2.50	1.52E-03	At1g23380	Homeobox transcription factor (KNAT6)	Regulation of transcription
2.42	4.94E-02	At3g58160	Myosin heavy chain, putative	Actin filament-based movement
2.39	3.62E-02	At1g23370	Homeobox transcription factor (KNAT6)	Regulation of transcription
2.30	7.34E-03	At2g22430	Homeobox-leucine zipper protein 6 (HB-6)	Regulation of transcription
2.27	2.95E-02	At4g01550	No apical meristem (NAM) family protein	Regulation of transcription
2.27	1.23E-02	At1g05570	Callose synthase 1 (CALS1)/1,3- β -glucan synthase 1	β -1,3 Glucan biosynthesis
2.06	1.62E-02	At1g52880	No apical meristem (NAM) family protein	Regulation of transcription
1.94	1.10E-04	At5g03455	GTPV2 (putative CDC25 homolog)	Protein amino acid phosphorylation
1.93	1.37E-02	At5g54310	ARF GAP-like zinc finger-containing protein ZIGA3 (ZIGA3)	Regulation of GTPase activity
1.92	1.72E-02	At3g55005	Tonneau 1b (TON1b)	Microtubule cytoskeleton organization and biogenesis
1.8	5.10E-03	At1g59610	Dynamin-like protein, putative (ADL3)	
1.71	2.30E-02	At4g29230	No apical meristem (NAM) family protein	Regulation of transcription
1.69	4.42E-02	At5g02470	DP-2 transcription factor, putative (DPA)	Regulation of progression through cell cycle
1.67	1.31E-02	At2g14120	Dynamin-like protein 2b (ADL2b/DRP2b)	
1.66	3.94E-02	At3g46010	Actin-depolymerizing factor 1 (ADF1)	Actin filament organization
1.64	3.64E-02	At1g14620	DECOY, endoxyloglucan transferase family (EXGT)	Biological process unknown
1.6	6.97E-03	At1g08620	Transcription factor jumonji (jmi) family protein	Regulation of transcription
1.6	7.02E-03	At5g43900	Myosin heavy chain (MYA2)	Actin filament-based movement

Data were obtained from the ATH1 microarray experiment with RNA from shoot apex of young plants grown under in vitro conditions. The P values were calculated according to a Bayesian test of linear model and corrected by the Holm's method.

position was confirmed by PCR (Table 4). The *hub2-1* plants were smaller, with pale green laminae and irregular blade surface, and their inflorescence stems were thinner than those of the Col stems and similar to those of *hub1-4* and *hub1-3* (Figure 1). The *hub2-1* mutation also reduced the rosette biomass to 43 and 42% of fresh and dry weight of Col, respectively (Figure 2B), and inhibited weakly, but significantly ($P < 0.001$), the root growth when the kinetic slopes of *hub2-1* and Col were compared (Figure 2C). Thus, organ growth was defective in the *hub2-1* and *hub1-1* mutants. The *hub2-1* mutation also modified the DNA ploidy level of leaf cells. Similar to *hub1-1*, the flow cytometry profile of *hub2-1* was slightly shifted in the G1-to-G2 cell populations in young leaves, and the endopolyploidy was higher than

that of the Col wild type with even 32C cells in mature leaves (see Supplemental Figure 2B online).

To determine whether HUB1 and HUB2 have a similar function, we analyzed the phenotype of homozygous double mutant plants. Reciprocal crosses of *hub2-1* to *hub1-3* were performed (Table 4). Double mutants were selected in the F2 based on their phenotypes, and the genotypes were verified in F3 progenies. No new leaf and flower phenotypes were observed, and the biomass of the double mutant lines fell statistically in the same group as that of both single parents (see Supplemental Figure 3 online). Therefore, HUB1 and HUB2 act in the same pathway.

The expression of the *HUB1* and *HUB2* genes monitored in different organs of *Ler* by quantitative RT-PCR indicated that the

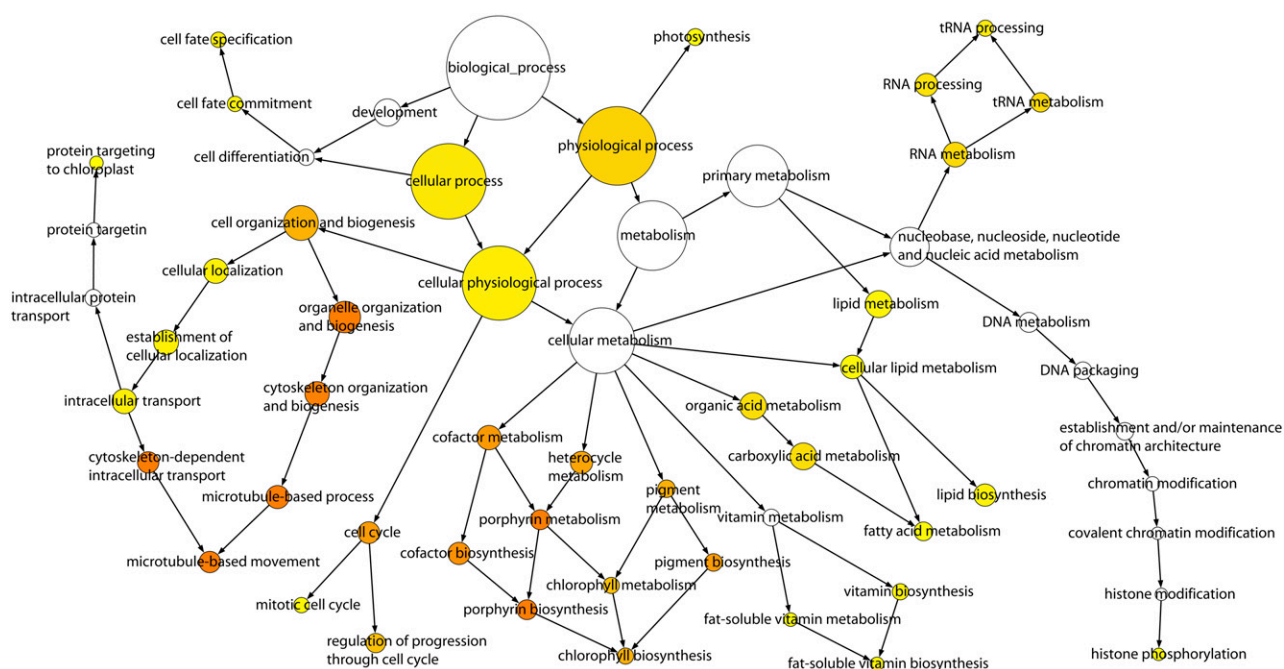


Figure 5. GO Analysis of 934 Downregulated Genes in Shoot Apices of *hub1-1* in the ATH1 Microarray Experiment.

The yellow to orange color of the circles correspond to the level of significance of the overrepresented GO category from 0.05 and below according to a multiple *t* test with false discovery rate-corrected *P* value. The size of the circle is proportional to the number of genes in the category.

genes were constitutively expressed in each plant organ examined as well as in synchronized cell cultures (data not shown). A search in Gene Atlas and Gene Chronologer of GENEVESTIGATOR also showed expression of *HUB1* (266817_at and 266818_at probe sets) and *HUB2* (259652_at and 259662_at probe sets) in all tissues and developmental stages (Zimmermann et al., 2004). According to a microarray analysis of leaf development (Beemster et al., 2005), the *HUB1* and *HUB2* genes were constitutively expressed during proliferation, expansion, and mature-stage phases of leaf and root development. Moreover, the expression level of both genes remained constant throughout the cell cycle (Menges et al., 2005). In conclusion, *HUB1* and *HUB2* are not temporally or spatially regulated at transcript levels.

HUB1 Protein Has Histone H2B Monoubiquitination Activity in Vitro

Based on sequence homologies, HUB1 had been previously identified as a BRE1 homolog (Hwang et al., 2003; Stone et al., 2005). To confirm the expected function of the HUB1 protein as H2B monoubiquitinating E3 ligase, a series of in vitro ubiquitination assays were performed. In such assays, functional BRE1 E3 ligase is expected to ligate one ubiquitin molecule on histone H2B, causing a corresponding increase in H2B molecular mass (Zhu et al., 2005). To this end, the cDNA-encoding HUB1 was expressed in *Escherichia coli* with a His tag for recombinant protein production and purification. The purified proteins were

refolded and subjected to in vitro assay with recombinant H2B, Rad6, E1, and HA-ubiquitin proteins. In the presence of all reagents, HUB1 mediated monoubiquitination of H2B (17 kD) that was seen as shift of H2B by 10 kD in the protein gel blot (Figure 6D). This band of 27 kD was reactive to both H2B-specific antibody and HA antibody that detected the HA-tagged ubiquitin. In the absence of E1, E2, or ubiquitin, no shift in H2B migration was seen. Similar results were obtained in ubiquitination reactions with glutathione S-transferase-tagged HUB1 (data not shown). Taken together, these data confirm that HUB1 is a functional ortholog of human and yeast BRE1 proteins.

DISCUSSION

***HUB1* Regulates Cell Proliferation during Early Leaf and Root Growth**

Our data showed that the *hub1-1* mutation had a negative effect on the growth and final size of leaves by impairing cell division activity. The intrinsic leaf size is determined by the number of cells produced by cell division activities during the early stages of primordium formation (Mizukami and Fischer, 2000). A group of genes have been reported to affect leaf shape and size by regulating cell numbers (Mizukami and Fischer, 2000; Nelissen et al., 2003, 2005; Horiguchi et al., 2005). However, another group of genes affect cell division, leaving organ growth relatively unaffected because of a compensatory effect by cell expansion

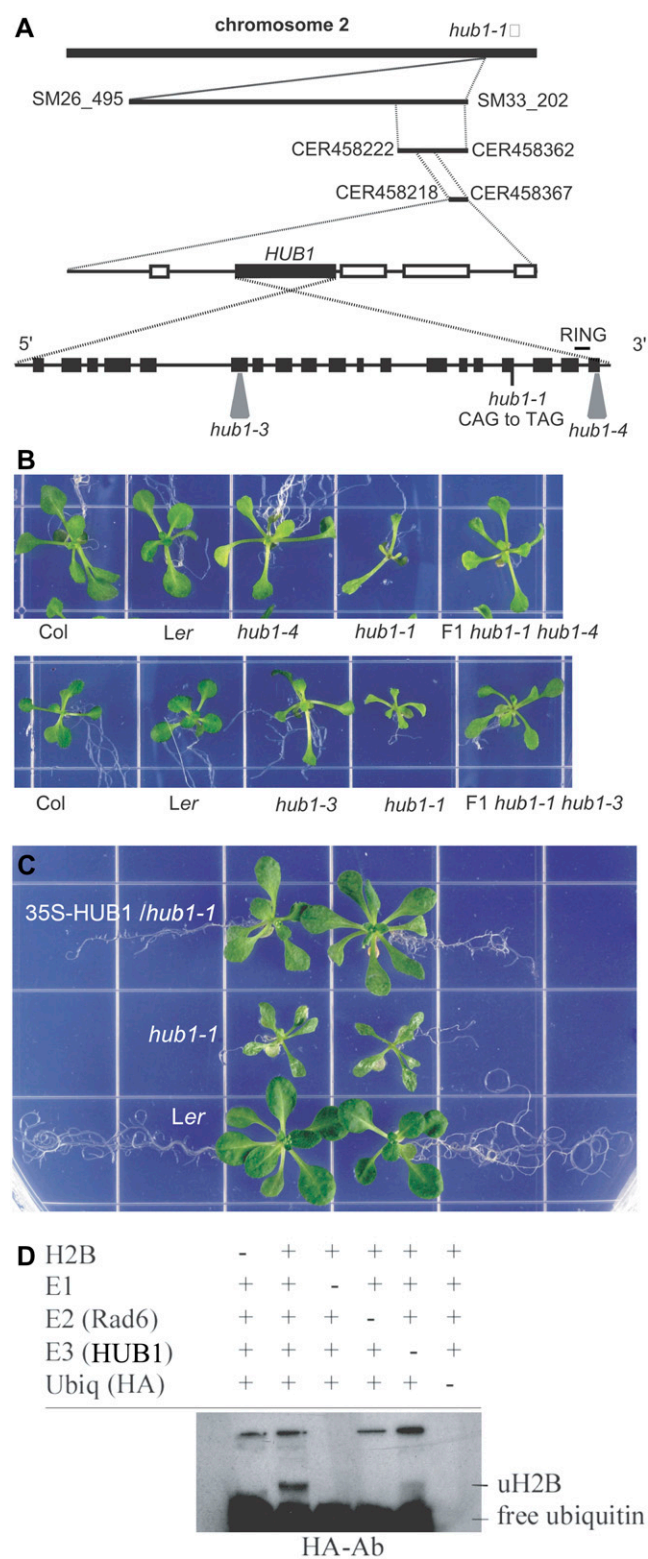


Figure 6. Identification of the *HUB1* Gene. **(A)** Map-based cloning strategy. Eight amplified fragment length polymorphism markers (SM) analyzed on 20 F2 phenotypically mutant plants identified the mutation in a 293-kb interval on chromosome 2. Recombination

(Hemerly et al., 1995; Autran et al., 2002), although the organ size rarely reaches completely that of the wild-type controls. The critical difference between these groups of genes appears to be how they affect the developmental timing of proliferation and differentiation phases. In *hub1-1*, the CDR was severely reduced during the early stage of leaf development because of the block at the G2-to-M transition and, consequently, prolonged cell cycle duration. However, the timing of cell proliferation and growth was not altered in the *hub1-1* mutant, and the leaf growth ceased by 18 DAS, similarly as in the wild type, thus, before the intrinsic organ size had been reached by the mutant. The primary cause of *hub1-1* phenotypes was due to the reduction of CDRs. Furthermore, although in the leaf sections of *hub1-1*, cell sizes were irregular, no compensation response was observed in the leaf epidermis. To verify whether these effects were similar in other organs and thereby explaining also the root phenotype of *hub1-1*, root kinematic analysis was done and confirmed that HUB1 regulates both shoot and root apical meristems and is apparently a general regulator of cell divisions. In contrast with single transcription factors regulating growth of a specific organ type, such as a leaf (Mizukami and Fischer, 2000; Horiguchi et al., 2005), HUB1 rather represents a regulator higher upstream from transcription factors and by its proposed function in chromatin activation might play a role in transcriptional programming for cell cycle progression and coordination of growth in multiple organ types.

HUB1 Affects G2-to-M Transition and Mitosis

The flow cytometry data of *hub1-1* leaves at early developmental stages indicated a G2-to-M block leading to a higher 4C/2C proportion than that of the wild type. As a consequence, the specific expression of genes during this phase of the cell cycle would be expected to be higher in proliferating tissues. By contrast, the microarray data showed a strong enrichment in M-phase-specific genes among those downregulated in the *hub1-1* mutant, namely, the A-type and B-type cyclins and three CDKBs that are key regulators in the G2-to-M transition (Inzé and De Veylder, 2006). These genes are actively repressed in the

binants used for fine-mapping delimited the locus to regions of 97 and 27 kb flanked by SNP markers (CER). The last interval of the 27-kb region contained four genes that were sequenced and allowed identification of the *hub1-1* mutation at the end of exon 16 of At2g44950, which was designated *HUB1*. Black boxes and triangles represent exons and T-DNA insertions, respectively. The RING domain position is indicated with a black line.

(B) Allelism test. Phenotype of the *hub1-1/hub1-4* and *hub1-1/hub1-3* heterozygotes grown in vitro, their respective parents, and the corresponding wild type (Ler for *hub1-1* and Col for *hub1-4* and *hub1-3*).

(C) Complementation test of the *hub1-1* mutant transformed with the p35S-*HUB1* construct.

(D) H2B ubiquitination assay by HUB1. Protein gel blot hybridization with HA antibody against HA-ubiquitin. Lane 1, no H2B substrate; lane 2, all components present; lane 3, no E1 enzyme; lane 4, no E2 (Rad6) enzyme; lane 5, no E3 HUB1; and lane 6, no ubiquitin.

Table 4. Alleles of the *HUB1* and *HUB2* Genes

Gene	Accession Number	Allele	Code	Genetic Background	Mutagen	Position of Mutation	Source
<i>HUB1</i>	At2g44950	<i>hub1-1 (ang4-1)</i>		<i>Ler</i>	EMS ^a	Exon 16	Berná et al. (1999)
		<i>hub1-4</i>	SALK_122512	Col	T-DNA	Exon 19	Alonso et al. (2003)
		<i>hub1-3</i>	GABI_276D08	Col	T-DNA	Exon 6	Rosso et al. (2003)
<i>HUB2</i>	At1g55250 and At1g55255	<i>hub2-1</i>	GABI_634H04	Col	T-DNA	Exon 13	Rosso et al. (2003)

^aEMS, ethyl methanesulfonate.

mutant, providing a potential molecular basis for the G2-to-M function of the HUB1 protein in transcriptional control of cell cycle genes. As a consequence of G2-to-M inhibition, a down-regulation of subsequent steps of mitosis would also be foreseen. The mitosis includes nuclear envelope breakdown, disassembly of the microtubule network and its rearrangement into mitotic spindles, chromatin condensation, and chromosome segregation before cytokinesis. Indeed, a high number of cytokinesis-related genes were differentially expressed in *hub1-1*. The most prominent group of downregulated genes encoded kinesins, which are motor proteins that carry cargo, such as vesicles. Of the 61 *Arabidopsis* genes encoding kinesins (Lee and Liu, 2004), 21 with a clear link to the cell division process were down-regulated in *hub1-1*, among which are *HINKEL/NACK1* and *TETRASPORE/NACK2*, *KNOLLE*, and *MAP/PLEIADE*. The *hinkel*, *tetraspore*, *knolle*, and *pleiade* knockout mutants are known to be defective in the cell plate formation during cytokinesis, leading to abnormal cells with often large nuclei (Müller et al., 2002; Strompen et al., 2002; Yang et al., 2003). The absence of a defect in root apical meristem organization in *hub1-1* is another argument for the mutation most probably affecting the entry into mitosis rather than the phragmoplast or cell plate formation itself.

The exit from the mitotic cell cycle coincides with the start of the endoreduplication, which can be unambiguously identified from the appearance of higher ploidy levels (>8C). In *hub1-1*, a proportion of cells exited the mitotic cycle very early; however, at the end of leaf development, 50% of the cells still remained with a 2C/4C content, suggesting that not all cells were stimulated to endoreduplicate. In wild-type leaves, the endoreduplication process starts after cessation of the mitotic cycle and when cells enter into the differentiation phase (Beemster et al., 2005). During development, a block of the G2-to-M transition may also result in an increased endoreduplication. For example, inhibition of CDKA activity at the G2-to-M transition by low overproduction levels of Kip-related protein 2 caused cells to enter prematurely into the endocycle (Verkest et al., 2005). Similarly, downregulation of CDKB1;1 activity by ectopic expression of its dominant-negative variant enhanced endoreduplication (Boudolf et al., 2004b). Thus, the enhanced level of endoreduplication in the *hub1-1* mutant probably resulted from the block in the G2-to-M transition suggested by flow cytometry data in combination with ongoing G1-to-S activity. Accordingly, the expression of the *SIM* gene, a repressor of mitosis during endoreduplication (Churchman et al., 2006), was enhanced in *hub1-1*, providing an additional component of the endoreduplication machinery affected by the mutation.

Phenotypes of the *hub1-1* Mutant Link the Plant BRE1 Ortholog to Cell Cycle Regulation

Mutation in the *HUB1* gene severely disrupted the cell division activities in the vegetative meristems investigated. Furthermore, the expression of several G2-to-M-specific genes was repressed in the mutants, indicating that the cell division defects were caused by active transcriptional effects. Several lines of evidence have linked BRE1 to cell cycle and growth regulation. In yeast, mutation in *BRE1* generates an enlarged cell phenotype, suggesting that H2B monoubiquitination is involved in cell size determination, perhaps through cell cycle-related transcriptional programming or START control (Hwang et al., 2003). In the *bre1* mutant of fruitfly, the Notch signaling is affected and causes defects in wing and leg growth (Bray et al., 2005). Furthermore, the activity of the Rad6/BRE1 protein complex appears to be regulated by a CDK protein (Wood et al., 2005). In yeast, *BUR1* is an essential gene encoding a *cdc28*-related CDK protein and *BUR2* is a cyclin, divergent from the cyclin T/C family. The BUR1/BUR2 complex functions in Rad6/BRE1 activation and affects several histone modifications involved in transcriptional elongation.

The mechanism by which BRE1 regulates the cell cycle might involve transcriptional programming. BRE1 mediates specifically the transcription activation functions of Rad6 (Wood et al., 2003; Kao et al., 2004). Monoubiquitination of H2B by BRE1 and Rad6 has been shown to be required for trimethylation of histone H3 at Lys-4 (H3K4met3) at coding sequences of transcriptionally active genes in yeast and humans (Wood et al., 2005; Xiao et al., 2005; Zhu et al., 2005; Shukla et al., 2006). This H3 modification is indispensable for RNA polymerase II recruitment to the coding sequences of transcribed genes. Recently, in genome-wide histone modification profiles, H3K4met3 modifications were associated with promoters of active genes that were either constitutively expressed or rapidly induced. The regulated genes included both cell cycle and developmental regulatory genes (Roh et al., 2006).

Other developmental mutants, such as *struwwelpeter* and *elongata*, have linked transcriptional programming or chromatin regulation with plant growth regulation (Autran et al., 2002; Nelissen et al., 2005). In addition to the severe cell division defects in the *hub1-1* mutant, a significant number of cell cycle genes were downregulated, suggesting that their misregulation caused the observed phenotypes. Thus, the transcriptional programming through chromatin activation appears to be an important part of the cell cycle regulation, and HUB1 might be one of the key players in the process.

METHODS

Plant Material and Growth Conditions

Seeds of *Arabidopsis thaliana* Ler and the *hub1-4* mutant (SALK_122512) were obtained from the Nottingham Arabidopsis Stock Centre. The *hub1-1* mutant has been described previously as *ang4-1* (Berná et al., 1999). The T-DNA insertion lines *hub1-3* (GABI_276D08) and *hub2-1* (GABI_634H04) were obtained from GABI-Kat.

The plants were generally grown in vitro on germination medium (Valvekens et al., 1988). For the microarray experiments, the medium used contained half-strength Murashige and Skoog salts (micro and macro elements), 1 g/L sucrose, 0.5 g/L 2-(*N*-morpholino)ethanesulfonic acid, pH 6.0, and 6 g/L plant tissue culture agar (Lab M). For root growth experiments, a single row of five plants was sown in square plates (BD Falcon) in vertical position in germination medium containing 10 g/L plant tissue culture agar (Lab M). The growth chamber conditions were 16-h-light/8-h-dark photoperiod with white light (cool-white neon tubes; Radium Lampenwerken), 100 $\mu\text{E M}^{-2} \text{ h}^{-1}$ photosynthetically active radiation, and 20°C. Plants were grown in a soil:vermiculite (3:1; v/v) mixture under greenhouse conditions with a setting temperature between 21 and 30°C, relative humidity of 50 to 60%, and the irradiance (natural light and fluorescent lamps) between 100 and 120 $\mu\text{E M}^{-2} \text{ h}^{-1}$ photosynthetically active radiation in a 16-h-light/8-h-dark regime.

Allele Characterization

The T-DNA alleles *hub1-4* (Alonso et al., 2003) and *hub1-3* (Rosso et al., 2003) of the *HUB1* gene (At2g44950) and the *hub2-1* (Rosso et al., 2003) allele of the *HUB2* gene (At1g55250 and At1g55255) were studied (<http://www.arabidopsis.org>). Their T-DNA insertion sites were verified by PCR on F2 plants with primers flanking the putative position of the T-DNA (P1 and P3) and a primer specific for the T-DNA left border (P2) (see Supplemental Table 1 online).

A dCAPS marker was designed for the *hub1-1* allele with the dCAPS finder program (<http://helix.wustl.edu/dcaps/dcaps.html>; Neff et al., 1998). The reverse primer 5'-CATACGGGCACACAGATATACCA-3' was designed by the program and contained a base change from T to A (underlined) to create a *Bgl*II restriction site in the Ler wild-type PCR product. The forward primer (5'-CATCAAGGTATCGTGTCCAACTC-3') was designed in the *HUB1* sequence to generate a PCR product of 406 bp. The *Bgl*II restriction would reduce the fragment with 20 bp; Ler and Col and the *hub1-4* and *hub1-3* alleles were wild type for this fragment. In the *hub1-1* allele, there was a point mutation at the created *Bgl*II site, thereby destroying it and resulting in an uncut PCR fragment. The PCR was performed as described by Neff et al. (1998). The PCR products were digested with *Bgl*II and run in a 3% agarose gel. In the F1 individuals that had been derived from crosses performed for allelism tests, two bands were amplified: a cut, wild-type fragment indicating the presence of the *hub1-4* or the *hub1-3* allele and an uncut fragment corresponding to the *hub1-1* allele.

Morphological and Histological Analysis

The expanded first three leaves of Ler and *hub1-1* plants grown in vitro were harvested at 30 and 40 DAS, respectively. Petiole, lamina, leaf length, lamina width, and area of leaves were measured, and the number of cells and the cell area of the upper epidermis and palisade parenchyma were scored as described by Cnops et al. (2004). The fully expanded first and second leaves of Ler and *hub1-1* plants grown in vitro (26 DAS) were sectioned, and the number of palisade mesophyll cells was determined under a microscope from transverse sections at the widest part of the lamina (Cnops et al., 2004). The statistical significance of the mean differences ($P = 0.05$) was analyzed by *t* test with the 10.0.5 software (SPSS).

For the biomass, the fresh weight was measured of plants grown under greenhouse conditions and harvested at the developmental stage 6.00 after removing the root and the inflorescence (Boyes et al., 2001), and the dry weight was obtained after drying the rosette at 60°C for at least 1 week. The experimental design comprised three replicates corresponding to three pools of five to eight plants, and the experiment was repeated twice. The data were statistically analyzed with SPSS by analysis of variance with two-fixed factor (genotypes and experiment) and three replicates, Bartlett's test, and Duncan's pairwise comparison between genotypes. The equality of error variances was controlled by Levene's test ($P > 0.05$).

Flow Cytometry and Kinematic Analyses of Leaf and Root Growth

The flow cytometry and the kinematic analyses of leaf growth were performed on plants grown in vitro as described by Beemster et al. (2005). Two biological and three technical replicates were used at each time point for flow cytometry measurement on first leaves, hypocotyls, and roots. Leaf growth of *hub1-1* and Ler was analyzed on five plants from 5 to 28 DAS by measuring the total leaf blade area of all cells from the abaxial epidermis drawn with a drawing tube attached to the microscope, the total number of cells, and the number of guard cells. The average cell area was determined from the number and total area of drawn cells, and the total number of cells per leaf was calculated by dividing the leaf area by the average cell area (averaged between the apical and basal positions). Finally, the average CDR for the whole leaf was determined as the slope of the \log_2 -transformed number of cells per leaf, which was done with second-degree and seven-point differentiation formulas (Erickson, 1976).

For root growth analysis, every 2 d, the position of the root tip was marked on the plate over a period of 14 d. The slope of the root length kinetics was used for an analysis of variance with one fixed factor (genotype) and $n = 5$, a Bartlett's test, and a Duncan's pairwise comparison. For root kinematic analysis, root growth was marked daily on plates. The plates were photographed after 10 d of germination, and the root growth was measured with ImageJ 1.34s software (<http://rsb.info.nih.gov/ij/>) by calculating the distance between successive marks along the root axis. Subsequently, seedlings were fixed in 70% ethanol overnight, replaced by lactic acid, and stored at room temperature in the dark. Roots were mounted on microscope slides, cortex cells in the mature zone were visualized with Nomarski differential interference contrast optics, and cell lengths of >1200 cells per line were measured with the ScionImage program (WinNT version beta3b; Scion).

Map-Based Cloning Procedure

The DNA extraction, amplified fragment length polymorphism, InDel, and SNP analyses were done according to Cnops et al. (2004) and Peters et al. (2004). The *HUB1* locus was fine-mapped with the InDel and SNP markers (see Supplemental Table 1 online). The four candidate genes identified in the last mapping interval were amplified from DNA and cDNA and fully sequenced in at least three replicates to identify the base exchange in the *hub1-1* mutant compared with Ler (see Supplemental Table 2 online).

Microarray Analysis

For the microarray experiment, samples were collected from 180 plants per line (comprising shoot apex meristem and first and second leaf primordia at the petioleless stage) at the growth stage 1.0 (Boyes et al., 2001). The RNA was extracted with the TriZol method (Invitrogen). The microarray experiment was done by the VIB MicroArrays Facility (Leuven, Belgium; <http://www.microarrays.be/>) with the ATH1 chips (Affymetrix) of 23,800 probe sets designed for *Arabidopsis* (Nelissen et al., 2005).

The experimental design comprised three replicates of each genotype, with one replicate corresponding to one RNA extraction on an independent pool of plants. The raw data from the Affymetrix GeneChip arrays (CEL files) were normalized with the GC Robust Multi Array average method from affy and gcma packages of Bioconductor Project Release 1.4 (<http://www.bioconductor.org/>) with the R 1.9.0 software. Subsequently, probabilities for differential expression were done by means of a Bayesian *t* test with the limma library as described by Nelissen et al. (2005). The Holm (1979) method was used to control multiple testing errors. The differentially expressed genes were selected at $P < 0.05$ in the *t* test after Holm's *P* value adjustment. The number of expressed genes was calculated by comparing the perfect match and mismatch signals with the affy package. For analysis of significantly overrepresented GO categories among up- and downregulated genes, we used the BiNGO plugin for Cytoscape (<http://www.psb.ugent.be/cbd/papers/BiNGO/>; Maere et al., 2005).

Recombinant Protein Production and Purification

The cDNA-encoding HUB1 was cloned by Gateway technology to the pDEST17 vector (Invitrogen) that introduced an N-terminal His tag into the protein. This plasmid was expressed in the *Escherichia coli* strain BL21-SI (Invitrogen) for recombinant protein production and purification. Protein production was induced with 0.3 M NaCl, overnight, at room temperature. Most His-tagged proteins were found in insoluble form. Therefore, the cell pellets were dissolved in 6 M urea buffer (20 mM Tris, pH 8, and 0.5 M NaCl) and lysed by extensive sonication. The His-tagged proteins were bound to Ni-NTA beads (Invitrogen) for 2 h at 4°C, washed, and eluted according to Jones and Gellert (2003). After elution, the His-tagged protein was dialyzed with decreasing urea concentration. The His-HUB1 proteins were refolded, while binding to Ni-NTA beads in a similar buffer as described for glutathione S-transferase pull-down assay (Kim et al., 2005). The refolded proteins were subjected to the in vitro ubiquitination assay.

In Vitro Ubiquitination Assay

The refolded HUB1 proteins, while bound on Ni-NTA beads (Invitrogen), ubiquitinated in vitro in buffers and conditions similar to those described by Zhu et al. (2005). Recombinant H2B, Rad6 (human), E1 (rabbit), and HA-ubiquitin (human) proteins were used as reagents. As negative controls, each component was omitted once from the assay. The E1, E2 (Rad6), and HA-ubiquitin were purchased from Boston Biochemicals and the H2B from Roche Diagnostics. Ubiquitination reactions were run on 10 or 17% sodium dodecyl sulfate-polyacrylamide gel electrophoresis and blotted on Immobilon polyvinylidene difluoride membranes (Millipore). The His-HUB1 proteins were detected by penta/tetra His antibody (Qiagen), the unmodified H2B protein by H2B (FL-126)-specific polyclonal antibody (Santa Cruz Biotechnology), and the ubiquitinated H2B by HA antibody against HA-ubiquitin.

Accession Numbers

Microarray data are available via ArrayExpress (E-MEXP-300). The accession numbers of the genes are At2g44950 (*HUB1*), At1g55250, and At1g55255 (*HUB2*). The seed stock codes are *hub1-1* (originally described as *ang4-1*), SALK_122512 (*hub1-4*), GABI_276D08 (*hub1-3*), and GABI_634H04 (*hub2-1*).

Supplemental Data

The following materials are available in the online version of this article.

Supplemental Table 1. Oligonucleotides Used as Primers to Confirm the Presence of T-DNA Insertions in GABI and SALK Lines.

Supplemental Table 2. InDel Markers Used for the Fine-Mapping of *HUB1*.

Supplemental Figure 1. Confocal Microscopy of Root Tips.

Supplemental Figure 2. Flow Cytometry Analysis of Nuclear DNA Content in Different Tissues.

Supplemental Figure 3. Rosette Biomass of the *hub1-3 hub2-1* Double Mutants, Parents, and the Wild Type.

ACKNOWLEDGMENTS

We thank Jan Zethof, Wilson Ardiles-Diaz, Paul Van Hummelen, and the technicians of the MicroArrays Facility (Leuven, Belgium) for technical assistance. We also thank Martine De Cock and Karel Spruyt for help in preparing the manuscript and figures. This work was supported by the European Research Training Network HPRN-CT-2002-00267 (DAGO-LIGN). K.H. and H.N. are indebted to the Institute for the Promotion of Innovation by Science and Technology in Flanders for postdoctoral fellowships, T.M.B. to the European Union-Human Resources and Mobility for an Early Stage Training grant (MEST-CT-2004-514632), and S.A. to the "Vlaamse Interuniversitaire Raad" for an International Course PhD scholarship. S.M. is a research fellow of the Research Foundation-Flanders.

Received January 24, 2006; revised January 15, 2007; accepted February 6, 2007; published February 28, 2007.

REFERENCES

- Alonso, J.M., et al. (2003). Genome-wide insertional mutagenesis of *Arabidopsis thaliana*. *Science* **301**: 653–657.
- Autran, D., Jonak, C., Belcram, K., Beemster, G.T.S., Kronenberger, J., Grandjean, O., Inzé, D., and Traas, J. (2002). Cell numbers and elongation in *Arabidopsis*. A functional analysis of the *STRUW-WELPETER* gene. *EMBO J.* **21**: 6036–6049.
- Beemster, G.T.S., and Baskin, T.I. (1998). Analysis of cell division and elongation underlying the developmental acceleration of root growth in *Arabidopsis thaliana*. *Plant Physiol.* **116**: 1515–1526.
- Beemster, G.T.S., De Veylder, L., Vercruysse, S., West, G., Rombaut, D., Van Hummelen, P., Galichet, A., Gruissem, W., Inzé, D., and Vuylsteke, M. (2005). Genome-wide analysis of gene expression profiles associated with cell cycle transitions in growing organs of *Arabidopsis*. *Plant Physiol.* **138**: 734–743.
- Berná, G., Robles, P., and Micol, J.L. (1999). A mutational analysis of leaf morphogenesis in *Arabidopsis thaliana*. *Genetics* **152**: 729–742.
- Boudolf, V., Barrôco, R., de Almeida Engler, J., Verkest, A., Beeckman, T., Naudts, M., Inzé, D., and De Veylder, L. (2004a). B1-type cyclin-dependent kinases are essential for the formation of stomatal complexes in *Arabidopsis thaliana*. *Plant Cell* **16**: 945–955.
- Boudolf, V., Vlieghe, K., Beemster, G.T.S., Magyar, Z., Torres Acosta, J.A., Maes, S., Van Der Schueren, E., Inzé, D., and De Veylder, L. (2004b). The plant-specific cyclin-dependent kinase CDKB1;1 and transcription factor E2Fa-DPa control the balance of mitotically dividing and endoreduplicating cells in *Arabidopsis*. *Plant Cell* **16**: 2683–2692.
- Boyes, D.C., Zayed, A.M., Ascenzi, R., McCaskill, A.J., Hoffman, N.E., Davis, K.R., and Görlach, J. (2001). Growth stage-based phenotypic analysis of *Arabidopsis*: A model for high throughput functional genomics in plants. *Plant Cell* **13**: 1499–1510.
- Bray, S., Musisi, H., and Bienz, M. (2005). Bre1 is required for notch signaling and histone modification. *Dev. Cell* **8**: 279–286.

- Chin, L.-S., Vavalle, J.P., and Li, L. (2002). Staring, a novel E3 ubiquitin-protein ligase that targets syntaxin 1 for degradation. *J. Biol. Chem.* **277**: 35071–35079.
- Churchman, M.L., et al. (2006). SIAMESE, a plant-specific cell cycle regulator, controls endoreplication onset in *Arabidopsis thaliana*. *Plant Cell* **18**: 3145–3157.
- Clough, S.J., and Bent, A.F. (1998). Floral dip: A simplified method for *Agrobacterium*-mediated transformation of *Arabidopsis thaliana*. *Plant J.* **16**: 735–743.
- Cnops, G., Jover-Gil, S., Peters, J.L., Neyt, P., De Block, S., Robles, P., Ponce, M.R., Gerats, T., Micol, J.L., and Van Lijsebettens, M. (2004). The *rotunda2* mutants identify a role for the *LEUNIG* gene in vegetative leaf morphogenesis. *J. Exp. Bot.* **55**: 1529–1539.
- Conaway, R.C., Brower, C.S., and Conaway, J.W. (2002). Emerging roles of ubiquitin in transcription regulation. *Science* **296**: 1254–1258.
- Cookson, S.J., Van Lijsebettens, M., and Granier, C. (2005). Correlation between leaf growth variables suggest intrinsic and early controls of leaf size in *Arabidopsis thaliana*. *Plant Cell Environ.* **28**: 1355–1366.
- Donnelly, P.M., Bonetta, D., Tsukaya, H., Dengler, R.E., and Dengler, N.G. (1999). Cell cycling and cell enlargement in developing leaves of *Arabidopsis*. *Dev. Biol.* **215**: 407–419.
- Erickson, R.O. (1976). Modeling of plant growth. *Annu. Rev. Plant Physiol.* **27**: 407–434.
- Hemerly, A., de Almeida Engler, J., Bergounioux, C., Van Montagu, M., Engler, G., Inzé, D., and Ferreira, P. (1995). Dominant negative mutants of the Cdc2 kinase uncouple cell division from iterative plant development. *EMBO J.* **14**: 3925–3936.
- Himanen, K., Boucheron, E., Vanneste, S., de Almeida Engler, J., Inzé, D., and Beeckman, T. (2002). Auxin-mediated cell cycle activation during early lateral root initiation. *Plant Cell* **14**: 2339–2351.
- Holm, S. (1979). A simple sequentially rejective multiple test procedure. *Scand. J. Stat.* **6**: 65–70.
- Horiguchi, G., Kim, G.-T., and Tsukaya, H. (2005). The transcription factor AtGRF5 and the transcription coactivator AN3 regulate cell proliferation in leaf primordia of *Arabidopsis thaliana*. *Plant J.* **43**: 68–78.
- Hwang, W.W., Venkatasubrahmanyam, S., Ianculescu, A.G., Tong, A., Boone, C., and Madhani, H.D. (2003). A conserved RING finger protein required for histone H2B monoubiquitination and cell size control. *Mol. Cell* **11**: 261–266.
- Inzé, D., and De Veylder, L. (2006). Cell cycle regulation in plant development. *Annu. Rev. Genet.* **40**: 77–105.
- Jones, J.M., and Gellert, M. (2003). Autoubiquitylation of the V(D)J recombinase protein RAG1. *Proc. Natl. Acad. Sci. USA* **100**: 15446–15451.
- Kao, C.-F., Hillyer, C., Tsukuda, T., Henry, K., Berger, S., and Osley, M.A. (2004). Rad6 plays a role in transcriptional activation through ubiquitylation of histone H2B. *Genes Dev.* **18**: 184–195.
- Karimi, M., Inzé, D., and Depicker, A. (2002). GATEWAY vectors for *Agrobacterium*-mediated plant transformation. *Trends Plant Sci.* **7**: 193–195.
- Kim, J., Hake, S.B., and Roeder, R.G. (2005). The human homolog of yeast BRE1 functions as a transcriptional coactivator through direct activator interactions. *Mol. Cell* **20**: 759–770.
- Lee, Y.-R.J., and Liu, B. (2004). Cytoskeletal motors in *Arabidopsis*. Sixty-one kinesins and seventeen myosins. *Plant Physiol.* **136**: 3877–3883.
- Liu, Y., Koornneef, M., and Soppe, W. (2007). The absence of histone H2B monoubiquitination in the *Arabidopsis hub1 (rdo4)* mutant reveals a role for chromatin remodeling in seed dormancy. *Plant Cell* **19**: 433–444.
- Maere, S., Heymans, K., and Kuiper, M. (2005). *BiNGO*: A Cytoscape plugin to assess enrichment of Gene Ontology categories in Biological Networks. *Bioinformatics* **21**: 3448–3449.
- Menges, M., de Jager, S.M., Gruijssem, W., and Murray, J.A.H. (2005). Global analysis of the core cell cycle regulators of *Arabidopsis* identifies novel genes, reveals multiple and highly specific profiles of expression and provides a coherent model for plant cell cycle control. *Plant J.* **41**: 546–566.
- Mizukami, Y., and Fischer, R.L. (2000). Plant organ size control: *AINTEGUMENTA* regulates growth and cell numbers during organogenesis. *Proc. Natl. Acad. Sci. USA* **97**: 942–947.
- Müller, S., Fuchs, E., Ovecka, M., Wysocka-Diller, J., Benfey, P.N., and Hauser, M.-T. (2002). Two new loci, *PLEIADE* and *HYADE*, implicate organ-specific regulation of cytokinesis in *Arabidopsis*. *Plant Physiol.* **130**: 312–324.
- Neff, M.M., Neff, J.D., Chory, J., and Pepper, A.E. (1998). dCAPS, a simple technique for the genetic analysis of single nucleotide polymorphisms: Experimental applications in *Arabidopsis thaliana* genetics. *Plant J.* **14**: 387–392.
- Nelissen, H., Clarke, J.H., De Block, M., De Block, S., Vanderhaeghen, R., Zielinski, R.E., Dyer, T., Lust, S., Inzé, D., and Van Lijsebettens, M. (2003). DRL1, a homolog of the yeast TOT4/KTI12 protein, has a function in meristem activity and organ growth in plants. *Plant Cell* **15**: 639–654.
- Nelissen, H., Fleury, D., Bruno, L., Robles, P., De Veylder, L., Traas, J., Micol, J.L., Van Montagu, M., Inzé, D., and Van Lijsebettens, M. (2005). The *elongata* mutants identify a functional Elongator complex in plants with a role in cell proliferation during organ growth. *Proc. Natl. Acad. Sci. USA* **102**: 7754–7759.
- Peeters, A., Blankstijn-de Vries, H., Hanhart, C.J., Léon-Kloosterziel, K.M., Zeevaert, J.A.D., and Koornneef, M. (2002). Characterization of mutants with reduced seed dormancy at two novel *rdo* loci and a further characterization of *rdo1* and *rdo2* in *Arabidopsis*. *Physiol. Plant.* **115**: 604–612.
- Pérez-Pérez, J.M., Ponce, M.R., and Micol, J.L. (2004). The *ULTRA-CURVATA2* gene of *Arabidopsis* encodes an FK506-binding protein involved in auxin and brassinosteroid signaling. *Plant Physiol.* **134**: 101–117.
- Peters, J.L., Cnops, G., Neyt, P., Zethof, J., Cornelis, K., Van Lijsebettens, M., and Gerats, T. (2004). An AFLP-based genome-wide mapping strategy. *Theor. Appl. Genet.* **108**: 321–327.
- Pye, K.A., Marrison, J.L., and Leech, R.M. (1991). Temporal and spatial development of the cells of the expanding first leaf of *Arabidopsis thaliana* (L.) Heynh. *J. Exp. Bot.* **42**: 1407–1416.
- Robles, P., and Micol, J.L. (2001). Genome-wide linkage analysis of *Arabidopsis* genes required for leaf development. *Mol. Genet. Genomics* **266**: 12–19.
- Roh, T.-Y., Cuddapah, S., Cui, K., and Zhao, K. (2006). The genomic landscape of histone modifications in human T cells. *Proc. Natl. Acad. Sci. USA* **103**: 15782–15787.
- Rosso, M.G., Li, Y., Strizhov, N., Reiss, B., Dekker, K., and Weisshaar, B. (2003). An *Arabidopsis thaliana* T-DNA mutagenized population (GABI-Kat) for flanking sequence tag-based reverse genetics. *Plant Mol. Biol.* **53**: 247–259.
- Schnell, J.D., and Hicke, L. (2003). Non-traditional functions of ubiquitin and ubiquitin-binding proteins. *J. Biol. Chem.* **278**: 35857–35860.
- Shukla, A., Stanojevic, N., Duan, Z., Shadle, T., and Bhaumik, S.R. (2006). Functional analysis of H2B-Lys-123 ubiquitination in regulation of H3-Lys-4 methylation and recruitment of RNA polymerase II at the coding sequences of several active genes *in vivo*. *J. Biol. Chem.* **281**: 19045–19054.
- Smalle, J., and Vierstra, R.D. (2004). The ubiquitin 26S proteasome proteolytic pathway. *Annu. Rev. Plant Biol.* **55**: 555–590.
- Stone, S.L., Hauksdóttir, H., Troy, A., Herschleb, J., Kraft, E., and Callis, J. (2005). Functional analysis of the RING-type ubiquitin ligase family of *Arabidopsis*. *Plant Physiol.* **137**: 13–30.

- Strompen, G., El Kasmi, F., Richter, S., Lukowitz, W., Assaad, F.F., Jürgens, G., and Mayer, U.** (2002). The *Arabidopsis* *HINKEL* gene encodes a kinesin-related protein involved in cytokinesis and is expressed in a cell cycle-dependent manner. *Curr. Biol.* **12**: 153–158.
- Valvekens, D., Van Montagu, M., and Van Lijsebettens, M.** (1988). *Agrobacterium tumefaciens*-mediated transformation of *Arabidopsis thaliana* root explants by using kanamycin selection. *Proc. Natl. Acad. Sci. USA* **85**: 5536–5540.
- Verkest, A., de O. Manes, C.L., Vercruysse, S., Maes, S., Van Der Schueren, E., Beeckman, T., Genschik, P., Kuiper, M., Inzé, D., and De Veylder, L.** (2005). The cyclin-dependent kinase inhibitor KRP2 controls the onset of the endoreduplication cycle during *Arabidopsis* leaf development through inhibition of mitotic CDKA1 kinase complexes. *Plant Cell* **17**: 1723–1736.
- Wood, A., Krogan, N.J., Dover, J., Schneider, J., Heidt, J., Boateng, M.A., Dean, K., Golshani, A., Zhang, Y., Greenblatt, J.F., Johnston, M., and Shilatifard, A.** (2003). Bre1, an E3 ubiquitin ligase required for recruitment and substrate selection of Rad6 at a promoter. *Mol. Cell* **11**: 267–274.
- Wood, A., Schneider, J., Dover, J., Johnston, M., and Shilatifard, A.** (2005). The Bur1/Bur2 complex is required for histone H2B mono-ubiquitination by Rad6/BRE1 and histone methylation by COMPASS. *Mol. Cell* **20**: 589–599.
- Wyrzykowska, J., Pien, S., Shen, W.H., and Fleming, A.J.** (2002). Manipulation of leaf shape by modulation of cell division. *Development* **129**: 957–964.
- Xiao, T., Kao, C.-F., Krogan, N.J., Sun, Z.-W., Greenblatt, J.F., Osley, M.A., and Strahl, B.D.** (2005). Histone H2B ubiquitylation is associated with elongating RNA polymerase II. *Mol. Cell. Biol.* **25**: 637–651.
- Yang, C.-Y., Spielman, M., Coles, J.P., Li, Y., Ghelani, S., Bourdon, V., Brown, R.C., Lemmon, B.E., Scott, R.J., and Dickinson, H.G.** (2003). *TETRASPORE* encodes a kinesin required for male meiotic cytokinesis in *Arabidopsis*. *Plant J.* **34**: 229–240.
- Zhu, B., Zheng, Y., Pham, A.-D., Mandal, S.S., Erdjument-Bromage, H., Tempst, P., and Reinberg, D.** (2005). Monoubiquitination of human histone H2B: The factors involved and their roles in *HOX* gene regulation. *Mol. Cell* **20**: 601–611.
- Zimmermann, P., Hirsch-Hoffmann, M., Hennig, L., and Gruissem, W.** (2004). GENEVESTIGATOR. *Arabidopsis* microarray database and analysis toolbox. *Plant Physiol.* **136**: 2621–2632.